

Distributed Acoustic Sensing Turns Fiber-Optic Cables into Sensitive Seismic Antennas

Zhongwen Zhan^{*1}

Abstract

Distributed acoustic sensing (DAS) is a new, relatively inexpensive technology that is rapidly demonstrating its promise for recording earthquake waves and other seismic signals in a wide range of research and public safety arenas. It should significantly augment present seismic networks. For several important applications, it should be superior. It employs ordinary fiber-optic cables, but not as channels for data among separate sophisticated instruments. With DAS, the hair-thin glass fibers themselves are the sensors. Internal natural flaws serve as seismic strainmeters, kinds of seismic detector. Unused or dark fibers are common in fiber cables widespread around the globe, or in dedicated cables designed for special application, are appropriate for DAS. They can sample passing seismic waves at locations every few meters or closer along paths stretching for tens of kilometers. DAS arrays should enrich the three major areas of local and regional seismology: earthquake monitoring, imaging of faults and many other geologic formations, and hazard assessment. Recent laboratory and field results from DAS tests underscore its broad bandwidth and high-waveform fidelity. Thus, while still in its infancy, DAS already has shown itself as the working heart—or perhaps ear drums—of a valuable new seismic listening tool. My colleagues and I expect rapid growth of applications. We further expect it to spread into such frontiers as ocean-bottom seismology, glacial and related cryoseismology, and seismology on other solar system bodies.

Cite this article as Zhan, Z. (2019). Distributed Acoustic Sensing Turns Fiber-Optic Cables into Sensitive Seismic Antennas, *Seismol. Res. Lett.* **91**, 1–15, doi: [10.1785/0220190112](https://doi.org/10.1785/0220190112).

Introduction

Seismic networks have existed for many decades. Each uses groups of seismic vibration sensors deployed with a wide range of extent or aperture, sensor density, and specific instrumentation. They have improved steadily. For example, the Southern California Seismic Network started with seven Wood–Anderson seismometers in the 1930s and comprises >400 high-quality broadband stations now. Seismologists have relied on them for answers to many questions and have gotten surprises in the process. Achievements include mapping the core-mantle boundary and charting the shallower Moho transition where crust meets mantle. At the local level, seismic stations and networks help chart faults and other geologic structures. These facilities handle signals from a vast range of events, from microseismicity that the citizenry never notices out to megathrust earthquakes that take lives, spawn tsunamis, flatten strong buildings, and send avalanches roaring downslopes. However, networks of often complex individual instruments are too costly to blanket the Earth's crust with them.

Seismology has found some shortcuts to high network density. The last decade saw a new trend to massing moderate quality “nodes,” such as stand-alone and rather simple geophones (e.g., [Hammond et al., 2019](#)). Portable nodal seismic networks can reveal striking complexities in basin structures, volcanoes, and fault zones (e.g., [Lin et al., 2013](#); [Schmandt and Clayton, 2013](#); [Ben-Zion et al., 2015](#); [Inbal et al., 2016](#); [Kiser et al., 2018](#); learn more in a recent *SRL* focus section on geophone array seismology prefaced by [Karplus and Schmandt, 2018](#)). In another recent effort to cut costs, seismic data from large numbers of tiny low-cost microelectromechanical systems (MEMS) accelerometers, including smartphones with built-in accelerometers, are now harvested by continuously running dense networks (e.g., [Cochran et al., 2009](#); [Clayton](#)

1. Seismological Laboratory, Division of Geological and Planetary Sciences, California Institute of Technology, Pasadena, California, U.S.A.

*Corresponding author: zwzhan@caltech.edu

© Seismological Society of America

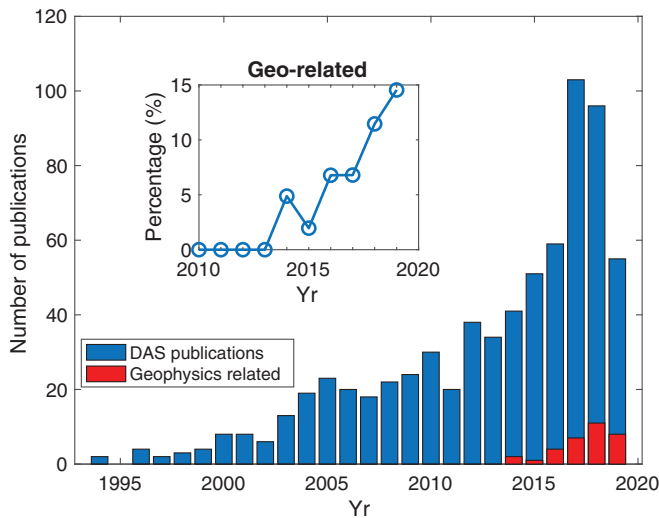


Figure 1. Trend of publications related to distributed acoustic sensing (DAS), according to the Web of Science (data accessed in July 2019). While the counts are likely incomplete (e.g., not including conference proceedings), there is a rapidly growing interest in DAS in the last few years. In the meanwhile, the applications of DAS in geoscience started around 2013–2014, and its share, although still small, increases rapidly and steadily since then (see the inset).

et al., 2015; Kong *et al.*, 2016; Inbal *et al.*, 2019). Distributed acoustic sensing (DAS), as do these examples, seeks to leverage existing technologies and infrastructure to gather more data despite strained budgets.

In essence, DAS provides a seismic sensor every few meters of a long optical fiber, currently out to tens of kilometers and limited by attenuation and nonlinearity of fibers. DAS starts by shining laser pulses into the fiber from one end. Rather than carrying data or other messages to a distant receiver or booster, as is standard for fiber optics, the front-end DAS apparatus interrogates an “echo” of the laser pulses. DAS makes it possible to deploy an ultra-dense array in dedicated fiber strands or to leverage pre-existing but idle telecommunication fiber strands. DAS was first employed by oil companies for exploration geophysics (e.g., Mestayer *et al.*, 2011; Daley *et al.*, 2013; Karrenbach *et al.*, 2018), and in the last few years it has expanded to serve regional and, at times, global seismological sciences (Fig. 1). Here, I will provide an overview of DAS and its impact on seismic networks. For pioneering use of DAS in the oil and gas industry, I defer to two recent special issues of *The Leading Edge* and *Interpretation* (prefaced by Willis *et al.*, 2017; Zhan *et al.*, 2019) and references therein.

What is DAS and How Does it Work?

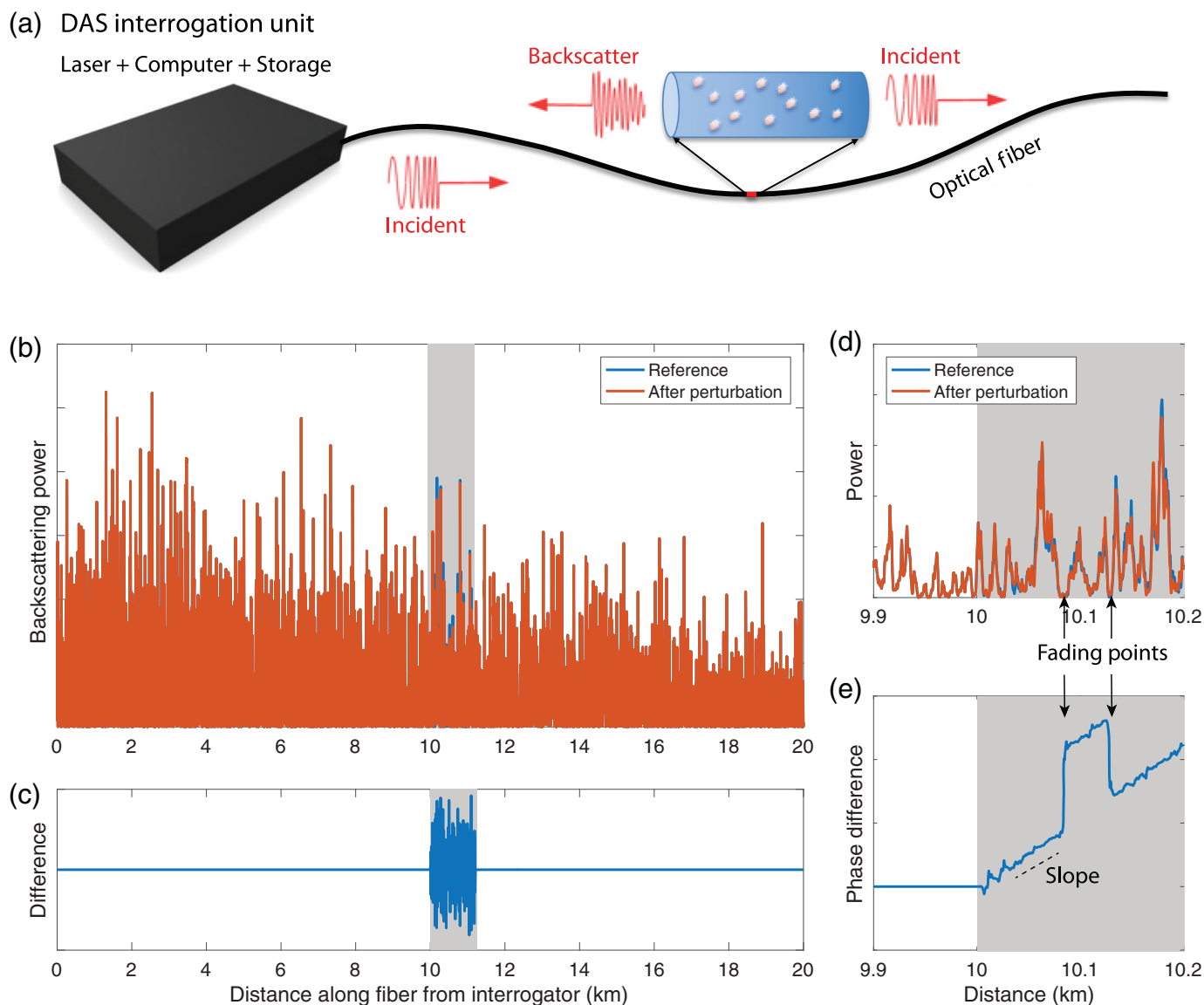
DAS belongs to a class of techniques called distributed fiber optic sensing (DFOS; Harrison, 1976; Hartog, 1983; Bao and Chen, 2012; Hartog, 2017), which includes variants such as

distributed temperature sensing (DTS) and distributed (static) strain sensing (DSS).

These techniques share a fundamental characteristic—rather than using fiber optics as passive infrastructure to transmit data from and among a string of complex and costly devices, the glass fibers are the sensors. DFOS exploits interaction of photons with intrinsic defects within a fiber, which are commonly fluctuations of refractive index in the glass. Each listening episode begins with a pulse of laser light sent down the fiber. The flaws scatter some of the light back to its source. A variety of scattering behaviors are sensitive to different kinds of outside influence on the fiber. DSS uses Brillouin scattering, DTS uses Raman or Brillouin scattering. A key point is that perturbations to the fiber due to variations in temperature, strain, or vibrations cause changes in the amplitude, frequency, or phase of light scattered back to the source.

In particular, DAS uses Rayleigh backscattering to infer the longitudinal strain (i.e., ϵ_{xx} with x along the cable) or strain change with time ($\dot{\epsilon}_{xx}$) every few meters along the fiber (Fig. 2). The strain in each fiber section changes when the cable is disturbed by seismic waves or other vibrations passing through the network. The return signals carry a signature of the disturbance. It takes only a slight extension or compression to a fiber to change the distances—as measured along the fiber—between many scattering points. The position changes are tiny, perhaps only a few tens of nanometers. The consequent alteration of flight return time of one point compared to others may only be fractions of a femtosecond. But interferometric analysis extracts how the signals from scattering points vary in timing or phase (Fig. 2). Further processing reconstructs with good fidelity the seismic waves behind the perturbation. DAS works even if the cable lies loose in a larger-diameter buried conduit, restrained only by friction with the conduit wall. As one would expect, tight coupling such as by bolting the cable casing fast to bed rock or packed regolith does improve the signal. DAS measures the changes by pulsing the laser thousands of times a second for tens of kilometers long fiber. This procedure, called phase-sensitive optical time-domain reflectometry, is the most widely used method in DAS (Masoudi and Newson, 2016). Several distinct system setups (e.g., dual-pulse, coherent detection, chirp-pulse) monitor the backscattered light. The principle is straightforward, and DAS is undergoing swift refinement. Key parameters such as sensing range, frequency band, measurement sensitivity, and gauge length vary substantially. I refer the readers to Hartog *et al.* (2013), Parker *et al.* (2014), Masoudi and Newson (2016), Hartog (2017), and Costa *et al.* (2019) for more technical details and some recent developments.

With a single engineered instrument connected at one end, and with natural scattering points used as seismic sensors every few meters or so and queried via laser, DAS provides dense arrays at low relative cost (Mateeva *et al.*, 2014; Lindsey *et al.*, 2017; Martin *et al.*, 2018). Although specially engineered fibers may boost backscattering and signal-to-noise ratios (e.g.,



Farhadiroushan *et al.*, 2019), DAS can also use regular telecommunication fiber cables that cost only dollars per meter. Such commercial cables may be ruggedized for various environments (e.g., high temperature, high abrasion). Figure 3a–c are examples of DAS arrays in dedicated fiber cables (e.g., Ajo-Franklin *et al.*, 2017; Dou *et al.*, 2017; Feigl and Team, 2017; Lindsey *et al.*, 2017; Zeng, Lancelle, *et al.*, 2017). DAS can also be applied to so-called dark fibers in pre-existing telecommunication cables that are not in use. This allows us to leverage large existing telecommunication fiber networks. This is a particularly attractive option in densely built-up urban areas as well as the deep sea floor (e.g., fiber map at Infrapedia; see Data and Resources). Fiber-optic cables are common in and around installations such as universities, research facilities, and large data centers. Figure 3d–f shows three examples of DAS arrays built upon pre-existing dark fibers, with apertures from 100s of meters to 10 km (e.g., Martin *et al.*, 2018; Ajo-Franklin *et al.*, 2019; Yu *et al.*, 2019).

Figure 2. Principles of DAS and a synthetic demonstration. (a) A DAS unit attaches to one end of a long optical fiber cable, sends laser pulses (harmonic or chirp) to the fiber, and interrogates the Rayleigh backscattered light from intrinsic fiber defects. The data processing and storage occur in real time within the DAS unit. (b) Synthetic time series of backscattering power, with the two-way time of flight converted to distance along fiber from the interrogator. The blue trace is the reference and the red is after applying a uniform strain to a ~1-kilometer-long section of fiber starting from 10 km (gray zone in all panels). (c) The changes in power due to the perturbation, that is, the difference between the two time series in (b). (d,e) Zoom into a 300 m section around 10 km, showing changes in power and phase, respectively. The slope of the phase differences quantitatively measures the magnitude of the applied along-fiber strain, zero before 10 km and constant after 10 km. The steps in (e), fading points, are caused by near-zero backscattering power and therefore uncertain measurements of phases. Fading points can be mitigated by multiple laser pulses with different frequencies or a chirp instead of harmonics (e.g., Costa *et al.*, 2019).

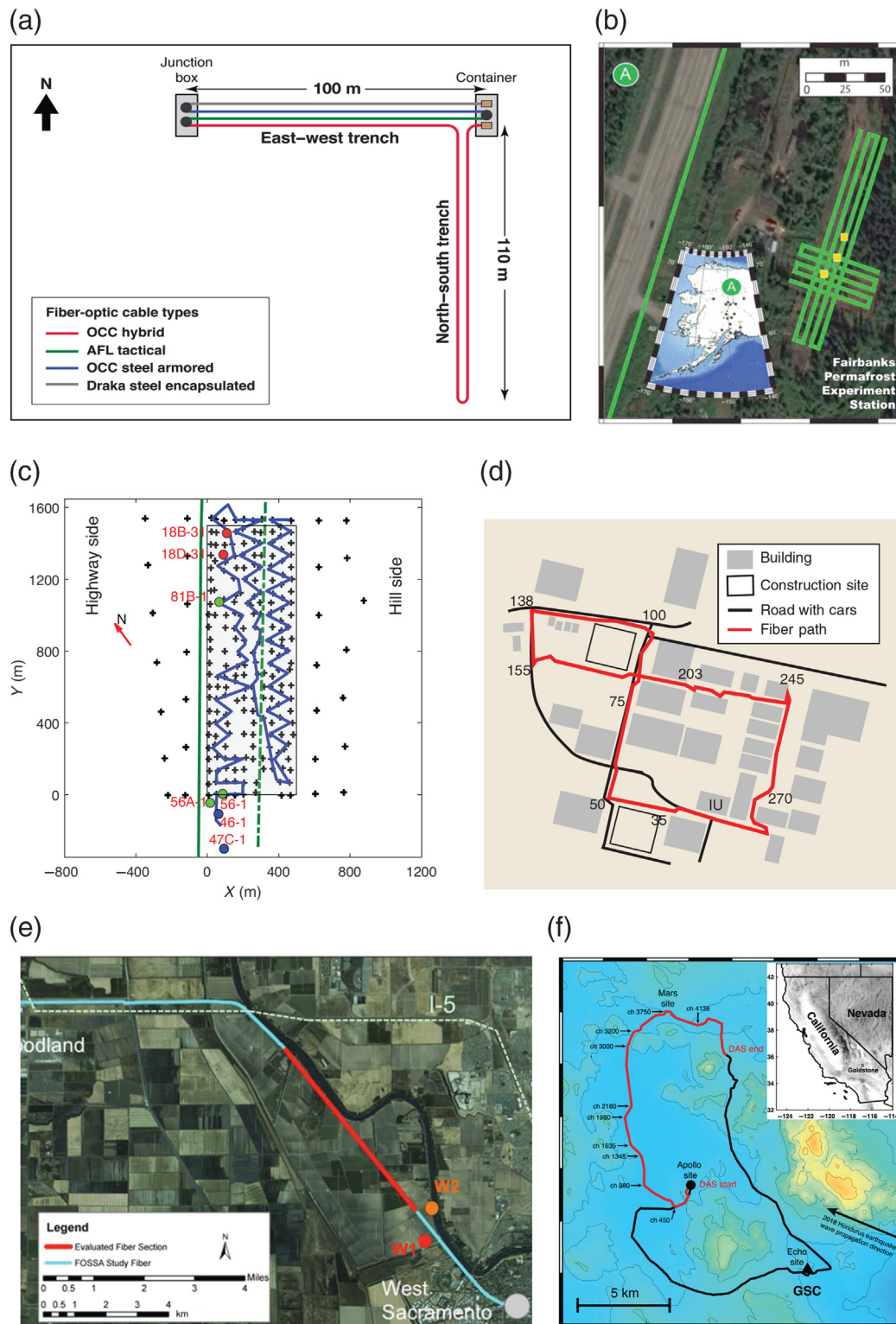
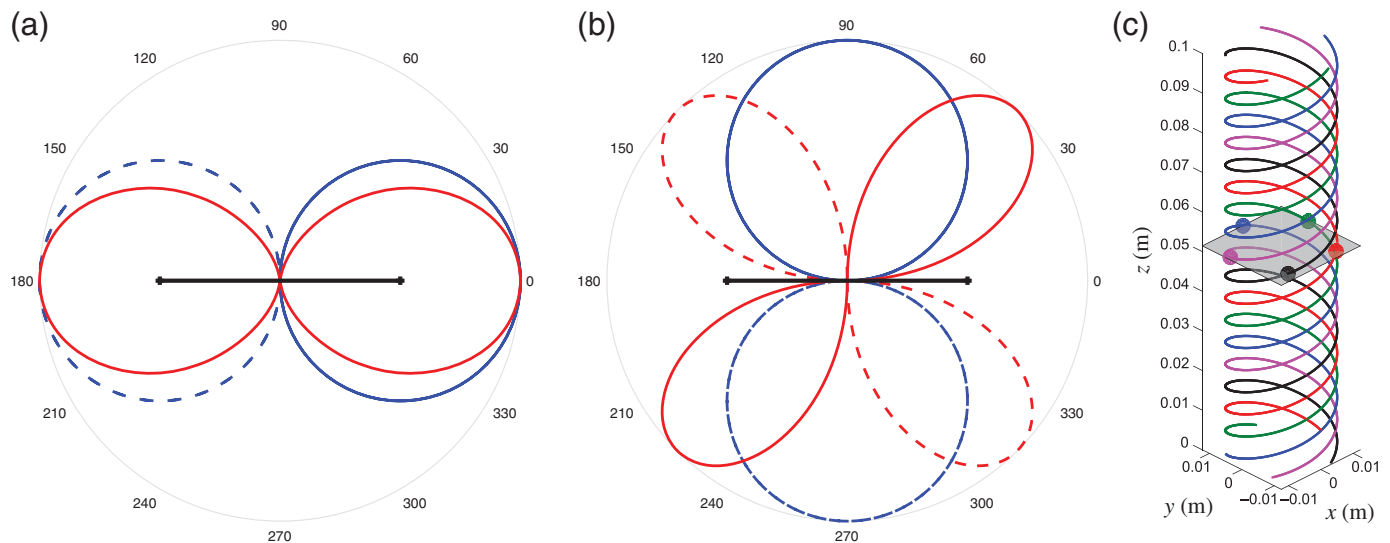


Figure 3. Recent examples of DAS arrays, using (a–c) dedicated fiber cables or (d–f) pre-existing telecom fiber cables. (a) A 100-m aperture “L”-shaped DAS array in Richmond, California, testing multiple types of fiber cables (figure from [Dou et al., 2017](#)). (b) [Ajo-Franklin et al. \(2017\)](#) constructed a DAS array in Alaska with a total of 7 km of fiber cable to monitor thawing of the permafrost layer. Inset map shows the location of the site. (c) The PoroTomo DAS array in the Bradly Spring geothermal field with about 8000 channels at 1 m spacing (figure from [Wang et al.,](#)

[2018](#)). (d) The Stanford DAS array using a 2-kilometer-long telecom fiber on the Stanford campus, continuously running since 2016 (figure from [Martin et al., 2018](#)). (e) A 20-kilometer-long DAS array using the ESNet dark fiber near Sacramento, California (red section; figure from [Ajo-Franklin et al., 2019](#)). (f) A 20-kilometer-long DAS array along the fiber cable connecting radio antennas in the National Aeronautics Space Administration Deep Space Network (red line; figure from [Yu et al., 2019](#)). FOSSA, GSC, OCC, AFL.



DAS Instrument Response and Data Quality

For a straight fiber section, DAS channels are approximately equivalent to linear strainmeters, first characterized by Benioff in 1935. Even though the principles are different (Rayleigh scattering in DAS vs. length changes between piers), DAS channels and the Benioff strainmeters share remarkably similar gauge lengths (~ 10 m) and directional sensitivity (Fig. 4). Natural seismic vibrations can have wavelengths from meters to thousands of kilometers. When the perturbing wavelength is much longer than the gauge length, DAS is highly sensitive to longitudinal waves propagating along the fiber and to transverse waves at 45° to the fiber. They are only weakly sensitive to broadside waves (Benioff, 1935; Papp *et al.*, 2017). Directional sensitivity to wavelengths comparable to the DAS gauge length is more complicated (Dean *et al.*, 2017; Martin *et al.*, 2019). To get around the challenge of low broadside sensitivity, some researchers propose and a few are testing helically wound fiber-optic cables (Fig. 4c; Kuvshinov, 2016; Hornman, 2017; Lim Chen Ning and Sava, 2018).

DAS's bandwidth, dynamic range, self-noise level, and many other capacities have not been as fully explored as they have for conventional seismometers (e.g., Clinton and Heaton, 2002) or strainmeters (e.g., Barbour and Agnew, 2011). This is due to such factors as laser noise, coupling among components, algorithm challenges, and the limited number of DAS seismology experiments so far. In laboratories, DAS has high sensitivity and broad bandwidth. For example, the iDAS technology from Silixa, Parker *et al.* (2014) achieved an 8 mHz–49.5 kHz bandwidth and 120 dB dynamic range from 5 nanostrain to 0.5% strain. More recently, Costa *et al.* (2019) reported picostrain/ $\sqrt{\text{Hz}}$ sensitivity at kHz frequencies in a well-controlled laboratory environment, using a chirp-based DAS system design. DAS performance in the field depends on many additional factors (e.g., cable type, coupling, and temperature stability).

Figure 4. (a) Red lines show directional sensitivity of DAS, or linear strainmeter in general, to P wave for a straight fiber section aligned along the horizontal axis (black lines). Solid and dashed lines mean positive and negative, respectively. Reproduced based on Benioff (1935). The directional sensitivity of a conventional seismometer's horizontal component is shown in blue lines as references. (b) Same as (a) but for S waves. (c) A helically wound fiber-optic cable design that can provide better broadside DAS sensitivity than straight fibers. Figure from Lim Chen Ning and Sava (2018).

Field DAS data quality compares well to records from collocated seismometers or geophones (e.g., Correa *et al.*, 2017). For an M_w 4.3 regional earthquake recorded on the PoroTomo DAS array at Brady Hot Springs, Nevada (its name a contraction of poroelastic tomography), Wang *et al.* (2018) showed wiggle-by-wiggle match between DAS and a nodal array, and with similar noise levels. Lindsey *et al.* (2017) summarized data from three DAS arrays and reported earthquake detections, mostly within a few hundreds of kilometers, with high signal-to-noise ratios and high-fidelity waveforms, and also the longer period waves from the 13 September 2016 M_w 5.8 Pawnee, Oklahoma, earthquake more than 2000 km away. Jousset *et al.* (2018) validated DAS amplitude response between 0.1 and 100 Hz with standard seismometers from the same locale. At even longer period and teleseismic distances, the 20 January 2018 M_w 7.5 Honduras earthquake produced high fidelity 0.02–1 Hz waveforms at the Goldstone DAS array near Barstow, California (Fig. 5; Yu *et al.*, 2019), although the noise on the DAS data was substantially higher than on a nearby broadband station. Becker *et al.* (2017) reported ~ 1 nm fracture displacement at milliHerz frequencies in a borehole DAS experiment.

One challenge distinctive to DAS data processing, especially with cables in existing infrastructure, is accurate plots of cable route. Although the flight time of laser pulses tells distance of measurements along fiber, the cables may have complex sags

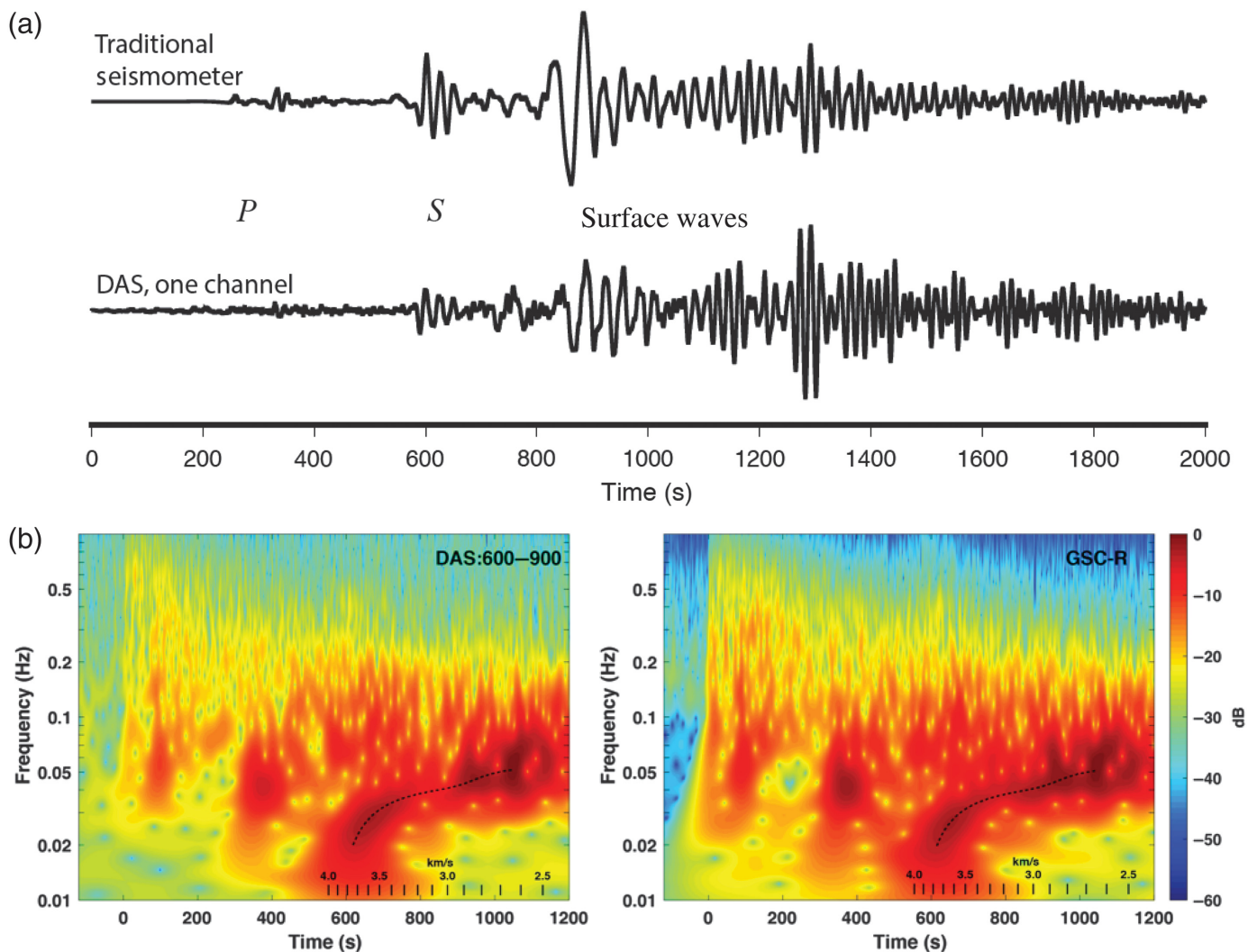


Figure 5. Broadband DAS waveforms of the 2018 M_w 7.5 Honduras earthquake on the Goldstone fiber seismic network (Fig. 3f), with an epicentral distance of about 40° . (a) Comparison of the radial-component waveform from a nearby broadband seismic station (CI.GSC) and the waveform at one DAS channel oriented in the radial direction. The P , S , and dispersive surface waves are all clear on the single DAS channel. The relative amplitude differences (e.g., stronger long-period surface waves around 850 s on GSC but stronger short-period surfaces on DAS) are due to the different sensitivities of particular motion velocity and strain (Yu et al., 2019). (b) Comparison of spectrograms from stacked DAS waveforms and GSC radial components shows that DAS can capture the correct frequency content in broadband and the dispersion too (dashed line). Figure from Yu et al. (2019).

or loops. With dedicated cables, tap tests along the cable as it is installed (e.g., sledge hammer blows mapped with Global Positioning System [GPS]) can provide coordinates of channels close to the tap points (e.g., Dou et al., 2017; Feigl and Team, 2017). Even then interpolation is necessary to map the channels between the tap points. Tap test can also be applied to portions of DAS networks on telecom dark fibers (e.g., Martin et al., 2018; Ajo-Franklin et al., 2019; Yu et al., 2019). But channels may be buried and access to private property is uncertain. Recently, Huot and Biondi (2018) applied machine learning to map DAS array geometry based on changes in wavefield features along cable. More accurate channel locations could improve the array-processing capability of DAS networks.

In summary, DAS has directional sensitivity comparable to linear strainmeters generally. It appears to have a broadband instrument response to strain or strain rate in the usual seismic frequency band and high-waveform fidelity. However, DAS's self-noise level so far has been substantially higher than that of broadband seismometers and is more comparable to geophones. Because of unknown coupling effects, the absolute amplitude may not be as accurate as the phase information.

For high-frequency applications (e.g., >10 Hz for shallow subsurface with slow seismic velocities), the seismic wavelength may be comparable or shorter than the DAS gauge length, and the response can be strongly frequency dependent. The quantification of DAS instrument response and data quality would benefit greatly from having more DAS networks and joint research efforts.

DAS in Local and Regional Seismology

Current DAS systems are already well suited for local and regional seismology. I now turn to DAS applications in three professional fields and discuss questions that DAS should help answer.

DAS in structure imaging and monitoring

Although we know that strong lateral heterogeneities of seismic structure (e.g., fault zones, basin edges, and Moho offsets) exist based on commonly observed scattered waves and multipathing effects, our current observations with traditional seismic networks are usually too aliased. Good maps of subsurface structures are important for understanding earthquake dynamics, prediction of ground shaking, and the flow or rheology of the crust and upper mantle. Capturing seismic wavefield portraits with large arrays is key to illuminating subsurface structures. An oil company's nodal seismic array near Long Beach with 5200 sensors within a 5 km × 10 km area was an eye-opener. In 2011, it revealed not only sharp velocity contrasts as seismic waves crossed faults and strong, shallow seismic anisotropies of other sorts, but also signs of a dramatic step in the Moho near the coast (e.g., [Lin et al., 2013](#); [Schmandt and Clayton, 2013](#)). Many subsequent temporary dense arrays (e.g., the Incorporated Research Institutions for Seismology [IRIS] community seismic network in Oklahoma, the San Jacinto fault array, and the iMush project on Mt. St. Helens) also demonstrated the benefits of unaliased portraits of wavefields (e.g., [Ben-Zion et al., 2015](#); [Hansen et al., 2016](#); [Kiser et al., 2018](#); [Sweet et al., 2018](#)).

Similarly, dense DAS arrays with their 1–10 m channel spacing can also provide unaliased sampling of seismic wavefields along fiber cables. The PoroTomo project surveyed signals from vibrating pads under heavy trucks, or vibroseis, with 8000 DAS channels and 200 nodes. The effort yielded high-resolution images of the top few hundred meters of soil and bedrock ([Parker et al., 2018](#); [Feigl et al., 2019](#)). Monitoring of ambient noise and other passive signals by multiple DAS arrays has recovered high-quality lower-frequency responses ([Lancelle, 2016](#); [Dou et al., 2017](#); [Zeng, Lancelle, et al., 2017](#); [Zeng, Thurber, et al., 2017](#); [Martin et al., 2018](#); [Ajo-Franklin et al., 2019](#)). With DAS arrays near busy roads such as PoroTomo, or in urban areas such as the Stanford array, common seismic noise, often from traffic and trains, can image shallow structures (e.g., [Ajo-Franklin et al., 2019](#)). To be sure, directional sensitivity of DAS and the varied and flexible geometry of fiber cables make DAS noise correlations substantially more challenging to decipher than such data from conventional seismometers (e.g., [Zeng, Lancelle, et al., 2017](#); [Martin et al., 2019](#)). Mitigation measures include correction for directional sensitivity ([Martin et al., 2019](#)) and full-waveform inversion for both Earth structure maps and noise source distribution ([Paitz et al., 2019](#)). Most DAS networks so far have been temporary deployments. They have not detected enough earthquakes for travel-time based tomography, which can

potentially resolve deep structures at a regional scale. But the data we do have is encouraging. Examples of local and regional earthquake detection on DAS (e.g., [Lindsey et al., 2017](#); [Wang et al., 2018](#)) show clean *P*- and *S*-wave onsets and complex coda wavefield, a set of data-rich intersecting waves that may echo and reflect inside the planet (e.g., [Fig. 6](#)). Because all the DAS channels along one cable share one GPS clock, there is great potential in using continuously running DAS arrays to improve travel time (absolute or differential) tomography in seismically active area (e.g., southern California). At longer period, [Yu et al. \(2019\)](#) extracted accurate 10–50 s dispersion curves from teleseismic, or distant-origin, surface waves captured on DAS. [Yu et al.](#) demonstrated teleseismic *P*-wave receiver functions on DAS by isolating the vertical component from a nearby three-axis station. Joint inversion of surface-wave dispersion curves, receiver functions are widely used by conventional networks to infer crust and upper-mantle structures. Larger-scale DAS networks can potentially revolutionize regional imaging of subsurface structures and geology.

Although some DAS arrays may not be in operation for long, their fibers are often left in place. This permits repeated or even permanent resumption of measurements to monitor seismic structure changes. Such 4D capability of DAS is already key in the petroleum industry to track fluid movements and geomechanical changes in the overburden for deep-water oil fields ([Mateeva et al., 2013, 2014](#)) and during hydraulic fracking or wastewater injection ([Byerley et al., 2018](#)). Recently, reflecting the widening use of DAS in research science, [Dou et al. \(2016\)](#) used it to monitor passive noise during human-induced thawing of permafrost in Alaska. They resolved changes as small as 2%. [Ajo-Franklin et al. \(2019\)](#) made highly repeatable measurements by noise interferometry for more than three months on the Sacramento DAS array, and plan to use it to monitor groundwater levels. [Biondi et al. \(2019\)](#) use closely located earthquakes recorded on DAS to chart shallow Earth structural changes below or abutting the Stanford campus. Potentially, the effort will detect a building foundation going in next to the fiber path. Similar to vibroseis trucks as repeating sources in 4D exploration seismology, permanent shakers (i.e., motors with eccentric weights) can repeatedly excite minutes to hours of harmonic waves or chirps detectable at large distances (e.g., [Ikuta, 2002](#); [Bradford et al., 2004](#); [Tanimoto and Okamoto, 2014](#)).

DAS in earthquake source studies

A central use of seismic networks is to monitor earthquakes of all sizes. Recent years have brought large improvements through denser networks and refinements such as template matching—recognition from archives of familiar kinds of pattern—and machine learning (e.g., [Shelly et al., 2007](#); [Peng and Zhao, 2009](#); [Ross, Trugman, et al., 2019](#)). In particular, large-*N* seismic arrays can now record an order of magnitude more events than cataloged by traditional seismic networks (e.g.,

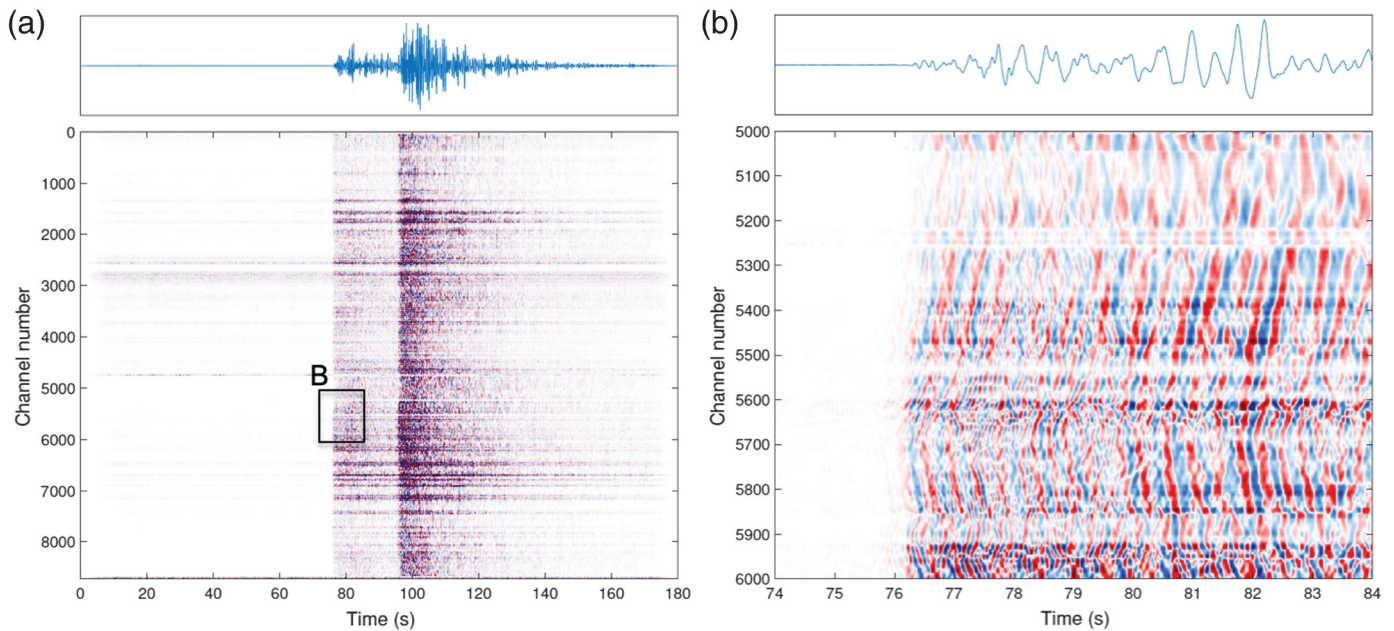


Figure 6. (a) Example DAS profile of an M_w 4.5 earthquake at regional distance, 150 km away. Data are from the PoroTomo project (Wang *et al.*, 2018). (b) A zoom-in of the P -wave window (rectangle in (a)), showing coherent tracking of the complex P wavefield along the fiber cable. This opens up the possibility of using not only the first arrivals but also the high-frequency coda waveform for studying the crust structures.

Inbal *et al.*, 2016; Li, Li, *et al.*, 2018; Li, Peng, *et al.*, 2018; Meng and Ben-Zion, 2018). However, nodal seismic arrays last untended for only a few weeks before batteries fade and data fills memory capacity.

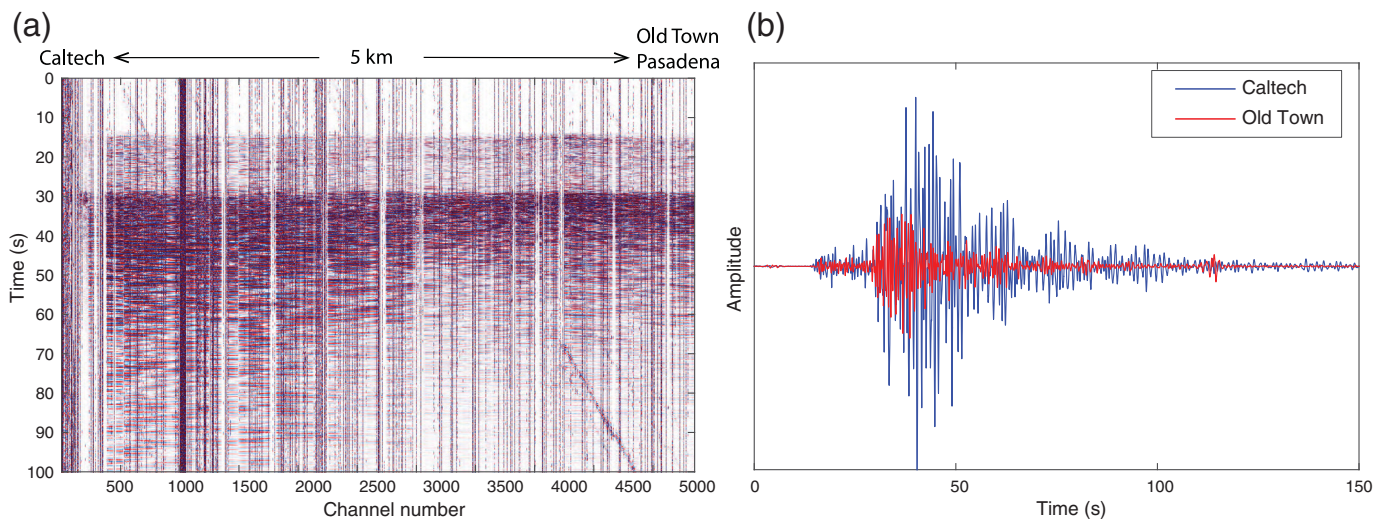
DAS arrays with even more sampling points by contrast can run without pause for extended periods, a benefit of having all power and data storage at the interrogator end. DAS networks thus have great monitoring potential, especially in urban areas with abundant fiber cables already in the ground. Lindsey *et al.* (2017) and Wang *et al.* (2018) showed that DAS channels clearly record seismic events at least as reliably as do conventional networks. Li and Zhan (2018) at the PoroTomo array, using templates of five cataloged events, detected 100 events in two weeks. They found tight correlation with industrial geothermal operations. Jousset *et al.* (2018) observed local earthquakes on a DAS array across faults with clear signatures of fault zones. Biondi *et al.* (2019) detected several events on the Stanford DAS array that had gone unrecorded by the local conventional network. DAS therefore seems able to improve sensitivity of earthquake detection by one to two magnitude units. Full realization of such potential cannot be instant. DAS arrays have not yet archived the years of earthquake waveform templates needed to train machines in assessing new events (e.g., Ross, Yue, *et al.*, 2019). Possible new approaches such as unsupervised machine learning and similarity-based algorithms may lead to effective DAS arrays as warning systems and with limited human labeling or other hands-on requirements (e.g., Li, Peng, *et al.*, 2018; Zhu and Beroza, 2018; Ross, Yue, *et al.*, 2019).

In a similar vein, DAS networks may also aid in prompt, accurate determination of such other source parameters as event location, focal mechanisms, and stress drop. Today, events close to detection threshold are hard to map. Only a

handful of stations may record clear signals. Data may thus suffer significant azimuth gaps in which events are recorded from just one or two distinct directions. DAS channels that are several kilometers long should substantially improve location accuracy for nearby events. Furthermore, dense arrays are better at recording earthquakes' radiation patterns to suggest a rupture's fault geometry and direction of slip (e.g., Fan and McGuire, 2018). Borehole DAS arrays that monitor microseismicity induced by hydraulic fracking have captured the nodal planes of P and S , as they emerge from events (e.g., Cole *et al.*, 2018). Such near-field seismic observation is a main reason for DAS's strength in exact recording of such vital parameters as radiated energy and stress drop. Along and near faults—including the San Andreas as an example in its early planning stages—DAS will provide invaluable data for understanding the physics of earthquakes and perhaps provide early public warnings as well (Karrenbach and Cole, 2016; Broderick *et al.*, 2019; Lapusta *et al.*, 2019, p. 78; Lellouch *et al.*, 2019).

DAS in hazard assessment and rapid responses

Seismic ground shaking varies widely even at equal distances from the source. Structural damage from one block to the next can be starkly different. Reasons include site effects in shallow sediment layers such as riverbed sediments that amplify



shaking under a house, that amplify shaking, 3D basin effects include reflection or conversion of waves interacting with basin edges, and nonlinearity of ground motion. For example, Clayton *et al.* (2012) measured peak ground acceleration from an M_w 2 earthquake next to the Long Beach array. Shaking in places was as much as five times greater than just a few hundred meters away. Efforts in understanding such complexity in seismic hazard assessment depend on dense-array observations, stochastic modeling efforts (e.g., Bowden *et al.*, 2015; Nakata *et al.*, 2015; Shi and Asimaki, 2018), and supercomputer simulation of high-frequency wave propagations (e.g., Graves and Pitarka, 2016). Soon after a large earthquake first responders urgently need to know where heavily damaged areas are most likely. One of the best tools for displaying such information is ShakeMap. It displays measured shaking intensity based on interpolation over seismic networks coupled with calculated site amplification estimates from shallow velocity models such as V_{S30} for shear wavespeeds in the top 30 m (Wald *et al.*, 1999; Worden *et al.*, 2010). However, reliability and resolution of ShakeMaps are limited by both station spacing gaps (e.g., 10–30 km for the Los Angeles area) and comparably sparse V_{S30} measurements (Yong *et al.*, 2016).

DAS arrays with their many channels and permanent nature are ideal for estimating shaking patterns and site responses at 10–100 m scales in urban areas. Their value is especially acute for key infrastructures that may already be connected by fiber (e.g., power plants, schools, and hospitals). With a prototype DAS array in the city of Pasadena, we recorded an M_w 4.5 earthquake at Cabazon, California, about 120 km away (Li *et al.*, 2019). Figure 7b shows the recorded section of waveforms along the 5-kilometer-long fiber path from California Institute of Technology’s (Caltech’s) campus to Old Town Pasadena. The P and S waves are clearly visible throughout the city, including stronger and longer shaking near Caltech. Figure 7c compares representative DAS seismograms from the transect—including a three-times-greater amplitude under and near the campus. We believe most of

Figure 7. (a) A ~5-kilometer-long DAS profile of shaking within the city of Pasadena, from California Institute of Technology (Caltech) to Old Town Pasadena, due to the 8 May 2018 M_w 4.5 Cabazon earthquake. Note that the shaking near the Caltech end of the fiber appears to be stronger and lasts longer too. This can be confirmed by comparing two representative DAS seismograms near the two ends in (b). Shaking near the Caltech end is about three times stronger. This difference could be caused by sediment thickness or local basin depths, although the fiber-ground coupling effects need to be address as well.

the observed contrast is rooted in basin geometry and perhaps site amplifications. However, we are pursuing more rigorous modeling of our DAS array to identify any artifacts due to fiber coupling and geometry.

Similar citywide DAS arrays (e.g., Ajo-Franklin *et al.*, 2019; Biondi *et al.*, 2019; Williams, Zhan, *et al.*, 2019) have detected many far-field moderate-size earthquakes. Seismic noise interferometry also mapped variation in site amplification, vital data for high-resolution ShakeMaps immediately after large earthquakes. A regional-scale DAS array, if operating when a big earthquake strikes, can be used directly in the making of the ShakeMap at much higher resolution, and may even contribute to faster early warnings. Data telemetry in DAS is near-real time and thus may trigger automated equipment to take lifesaving measures such as slowing trains and warning people off sidewalks and away from windows. For regions without DAS networks, it may still be worthwhile after a large earthquake to promptly adopt local underground fibers as DAS networks to monitor aftershocks that can be as or more damaging than an initial “mainshock” (e.g., the 2019 M_w 6.4 and M_w 7.1 Ridgecrest earthquakes on 4 and 5 July, respectively).

New Frontiers for Fiber Seismology

DAS shows tremendous promise beyond local and regional seismology. A short list of somewhat obvious new applications for DAS includes observing slow-moving landslides and active

volcanoes plus building low-maintenance networks in seismically quiet regions. A few exciting frontiers that await DAS merit more extended discussion.

Ocean-bottom fiber seismic networks

Earthquakes are mostly on or near plate boundaries. The most active plate margins are predominately in the world's ocean basins. They include the Cascadia subduction zone off the U.S. Pacific Northwest shore and such spreading centers as the Mid-Atlantic Ridge. But seismometers are mostly on land. This hinders seismologists seeking uniformly high-resolution global images of Earth's core and deep mantle, which are essential for answering fundamental geophysics questions. Furthermore, seismic monitoring of the ocean floor is critical to understanding how large earthquakes rupture. Many of the largest occur in submarine settings. Current and recent efforts to do seismology in the ocean floor use cabled observatories (e.g., the Ocean Observatories Initiative in the Cascadia subduction zone and the S-NET and DONET offshore Japan), and acoustically telemetered systems (e.g., [Frye et al., 2005](#); [Berger et al., 2016](#)), and floats (e.g., [Nolet et al., 2019](#)).

Thousands of miles of submarine optical fiber cables already cross the seafloor for telecommunication. Many have excess capacity. DAS can employ this idle and available infrastructure to fill many of the huge gaps in ocean-basin seismic coverage (e.g., [Hartog et al., 2018](#); [Hammond et al., 2019](#)). Particularly, geophysically interesting sites such as the Hawaii and Iceland hotspots and coastal cities next to subduction zones (e.g., Tokyo, Seattle, Lima) are also major onshore nodes for submarine fiber networks. Their radiating cables should thus help test important hypotheses pertaining to hot spot plumes and other immense but largely speculative mantle structures. DAS also could keep close watch for intimate details of great subduction zones near land as slabs of lithosphere lurching over and under one another generate potentially major earthquakes. Recently in a pioneering work, [Marra et al. \(2018\)](#) used hundreds of kilometers of seafloor fiber cables to detect submarine earthquakes, by interrogating the round-trip travel times of laser pulses with frequency metrology interferometric techniques. Their approach, which is different from DAS, has superior range and high sensitivity, but limited spatial resolution because the entire cable is a single integrated sensor. [Gutscher et al. \(2018\)](#) showed examples of DSS on the ocean floor by leveraging a 28-kilometer-long telecom fiber installed for a high-energy physics experiment. Recently, [Williams, Fernandez-Ruiz, et al. \(2019\)](#) converted a 40 km submarine fiber cable in water about 40 m deep offshore of Belgium into a DAS array with 4000 channels and 10 m spacing. It detected both large teleseismic earthquakes and how local ocean waves generated seismic noise at double frequency (i.e., secondary microseism). The SEA-bottom Fiber-Optic Observatory for Distributed measurements project, on the other hand, recorded small regional earthquakes in water up to 2500 m deep. It also demonstrated potential applications in

physical oceanography ([Sladen et al., 2019](#)). [Lindsey et al. \(2019\)](#) applied DAS to a 20-kilometer-long fiber cable at 20–50 m depth connected to the offshore Monterey Accelerated Research System node on the central California coast. They also reported detection of a regional earthquake, ocean waves, and seismic noise. These independent studies collectively show DAS starting to provide valuable data for submarine geophysics and physical oceanography. Although DAS may revolutionize seismology by expanding data coverage to the oceans, challenges remain on how to gain access to heavily used submarine cables. Also currently unclear is how to extend DAS' range from tens of kilometers to 1000 km or more to gain coverage across whole oceans.

Array seismology in planetary missions

Internal structures of the other terrestrial planets and the Moon are key to understand their and the Earth's formation and evolution. Constrained by technical difficulties and cost, planetary seismology has mostly been focusing on single devices (e.g., Viking, Mars Insight) or a few stations (e.g., Apollo). Meanwhile, Earth seismology relies heavily on seismic networks for almost any deep-geology study. DAS arrays could similarly answer many planetary seismology questions. Seismologists could use DAS arrays to better locate seismic events, conduct tomography of lateral variations, and inspect coda waves to reveal small-scale heterogeneities on moons and planets. Optical fiber cables can be made to survive harsh environments such as heavy dust, high temperature, and high radiation (e.g., [Daley et al., 2013](#); [Girard et al., 2013](#); [Feigl and Team, 2017](#)). The DAS units can be in landers or other shelters. For planets or moons with light atmosphere, a shallow burial of fiber cable may provide enough coupling, temperature buffering, and radiation shielding. Multiple 10–100-kilometer-aperture DAS arrays could revolutionize our understanding of other planets. However, current DAS instruments are not yet spaceproof. Just deploying fiber cable on another world may require advances in such fields as robotics. To fulfill this vision, we need to improve DAS sensitivity and sensing range while trimming system size and power demand.

DAS on glaciers

Interest in glacier seismology has surged since the early 2000s (see reviews by [Podolskiy and Walter, 2016](#); [Aster and Winberry, 2017](#)). Several permanent seismic networks are in Greenland and Antarctica where seismologists also conducted many brief seismic experiments. The remoteness and harsh environment in glacial regions makes seismic networks particularly expensive. Therefore, continuously operating dense seismic networks are rare. Nonetheless, the density, channel spacing, and broadband response of DAS make it a tantalizing way to study glaciers at different scales to explore such processes as iceberg calving, basal sliding, crevassing, and subglacial hydrology. As in the planetary mission scenario, engineers can

make fiber cable able to take harsh environments with power systems, sensitive electronics, laser, and data storage bundled at one end. We may also expect refreezing to provide coupling between fiber and ice, better than in typical DAS using cables loose in conduits (Castongia *et al.*, 2017). DAS can also be deployed down boreholes with hot-water drilling from the ice surface nearly to bedrock below. This would provide unique datasets to study near-field behavior of subglacial or englacial seismic events. As a plus, other fiber sensing techniques such as DTS (e.g., Kobs *et al.*, 2014) and DSS (e.g., Iten, 2011, for applications to landslides) can be combined in one borehole to measure both temperature and strain. Such setups could run continuously as observatories or be reoccupied as needed. The remoteness of most glaciers demands interrogation systems that can be powered by such means as batteries or solar panels. The significant deformation and crevassing of ice may impel use of cables that are not only very strong but also easy to deploy and perhaps to recover.

Conclusion

DAS provides an affordable and scalable way to deploy large-aperture, continuously running, and dense seismic arrays in locations difficult for traditional seismic instruments (e.g., urban areas, oceans, and planets). This opens up unprecedented opportunities for a wide range of seismology applications. While developed first for resource exploration and production geophysics, it is emerging strongly in fundamental research on earthquakes, our planet's deep structure, and seismic hazards. It holds promise in areas such as glaciology and planetary seismology. Several DAS networks with either dedicated fiber cables or existing telecommunication fiber cables have demonstrated the strong potential of DAS in local and regional seismology, such as in detection of microseismicity, mapping of shallow basin structures, monitoring changes in Earth structure, and seismic microzonation. In the meantime, DAS technology is improving rapidly through new designs of interrogator units, specialty fibers to achieve longer interrogation ranges, higher sensitivity, and lower noise. Although there are still challenges in storing and sharing DAS data (e.g., like what seismologists do through IRIS) and to understand DAS instrument response, DAS networks will inevitably become another important component of next-generation multiscale seismic networks with many different types of sensors (e.g., broadband, MEMs, nodes, smartphones, and smart devices). It is seismologists' job to incorporate all the available information seamlessly to address important geophysics questions.

Data and Resources

The information on Infrapedia can be found at <https://live.networkatlas.com> (last accessed April 2019). A video tutorial of DAS by Eileen Martin and Nate Lindsey is available on Youtube (<https://youtu.be/LAcQ44YRMuM>, last accessed October 2019). The PoroTomo data, including two weeks of DAS data, are openly

available on <http://gdr.openei.org/submissions/980> (last accessed October 2019) thanks to the PoroTomo team (University of Wisconsin, 2017). Please see Wang *et al.* (2019) for a report on the pre-AGU DAS workshop WS29: Distributed Acoustic Sensing: Principles and Case Studies, with a link to the materials presented.

Acknowledgments

This work is supported by California Institute of Technology–Jet Propulsion Laboratory (Caltech-JPL) President and Director's Fund, the Keck Institute for Space Studies, and the National Science Foundation (NSF) CAREER Award 1848166. The author benefited from discussions with Jonathan Ajo-Franklin, Biondo Biondi, Nate Lindsey, Eileen Martin, Miguel González Herráez, Fidalgo Martins Hugo, Martin Karrenbach, Thomas Coleman, Xiangfang Zeng, Mark Panning, Andrew Klesh, and Alireza Mirandi. The author thanks Duarte Pereira da Costa Luis for help preparing Figure 2. The author thanks two anonymous reviewers for helping clarify the article substantially, Charles Petit for editing the article, and Editor-in-Chief Zhigang Peng for inviting this contribution.

References

- Ajo-Franklin, J., S. Dou, T. Daley, B. Freifeld, M. Robertson, C. Ulrich, T. Wood, I. Eckblaw, N. Lindsey, and E. Martin (2017). Time-lapse surface wave monitoring of permafrost thaw using distributed acoustic sensing and a permanent automated seismic source, *SEG Technical Program Expanded Abstracts 2017*, Society of Exploration Geophysicists, 5223–5227.
- Ajo-Franklin, J. B., S. Dou, N. J. Lindsey, I. Monga, C. Tracy, M. Robertson, V. Rodriguez Tribaldos, C. Ulrich, B. Freifeld, T. Daley, *et al.* (2019). Distributed acoustic sensing using dark fiber for near-surface characterization and broadband seismic event detection, *Sci. Rep.* **9**, Article Number 1328, doi: [10.1038/s41598-018-36675-8](https://doi.org/10.1038/s41598-018-36675-8).
- Aster, R. C., and J. P. Winberry (2017). Glacial seismology, *Rep. Prog. Phys.* **80**, no. 12, 126801, doi: [10.1088/1361-6633/aa8473](https://doi.org/10.1088/1361-6633/aa8473).
- Bao, X., and L. Chen (2012). Recent progress in distributed fiber optic sensors, *Sensors* **12**, no. 7, 8601–8639, doi: [10.3390/s120708601](https://doi.org/10.3390/s120708601).
- Barbour, A. J., and D. C. Agnew (2011). Noise levels on plate boundary observatory borehole strainmeters in southern California, *Bull. Seismol. Soc. Am.* **101**, no. 5, 2453–2466, doi: [10.1785/0120110062](https://doi.org/10.1785/0120110062).
- Becker, M. W., C. Ciervo, M. Cole, T. Coleman, and M. Mondanos (2017). Fracture hydromechanical response measured by fiber optic distributed acoustic sensing at milliHertz frequencies: Fracture hydromechanics from DAS, *Geophys. Res. Lett.* **44**, no. 14, 7295–7302, doi: [10.1002/2017GL073931](https://doi.org/10.1002/2017GL073931).
- Benioff, H. (1935). A linear strain seismograph, *Bull. Seismol. Soc. Am.* **25**, no. 4, 283–309.
- Ben-Zion, Y., F. L. Vernon, Y. Ozakin, D. Zigone, Z. E. Ross, H. Meng, M. White, J. Reyes, D. Hollis, and M. Barklage (2015). Basic data features and results from a spatially dense seismic array on the San Jacinto fault zone, *Geophys. J. Int.* **202**, no. 1, 370–380, doi: [10.1093/gji/ggv142](https://doi.org/10.1093/gji/ggv142).
- Berger, J., G. Laske, J. Babcock, and J. Orcutt (2016). An ocean bottom seismic observatory with near real-time telemetry, *Earth Space Sci.* **3**, no. 2, 68–77.

- Biondi, B., S. Yuan, E. Martin, F. Huot, and R. Clapp (2019). *Using Telecommunication Fiber Infrastructure for Earthquake Monitoring and Near-Surface Characterization*, AGU Books.
- Bowden, D. C., V. C. Tsai, and F. C. Lin (2015). Site amplification, attenuation, and scattering from noise correlation amplitudes across a dense array in Long Beach, CA, *Geophys. Res. Lett.* **42**, no. 5, 1360–1367.
- Bradford, S. C., J. F. Clinton, J. Favela, and T. H. Heaton (2004). Results of Millikan Library forced vibration testing, *Technical Report EERL 2004-03*.
- Broderick, N., J. Loveday, K. van Wijk, J. Townend, and R. Sutherland (2019). *Optical Measurements of Temperature and Strain of New Zealand's Alpine Fault*, 2019 SSA Annual Meeting, Seattle, Washington, 27–30 April.
- Byerley, G., D. Monk, P. Aaron, and M. Yates (2018). Time-lapse seismic monitoring of individual hydraulic frac stages using a down-hole DAS array, *The Leading Edge* **37**, no. 11, 802–810, doi: [10.1190/tle37110802.1](https://doi.org/10.1190/tle37110802.1).
- Castongia, E., H. F. Wang, N. Lord, D. Fratta, M. Mondanos, and A. Chalarí (2017). An experimental investigation of distributed acoustic sensing (DAS) on Lake Ice, *J. Environ. Eng. Geophys.* **22**, no. 2, 167–176, doi: [10.2113/JEEG22.2.167](https://doi.org/10.2113/JEEG22.2.167).
- Clayton, R. W., T. Heaton, M. Chandy, A. Krause, M. Kohler, J. Bunn, R. Guy, M. Olson, M. Faulkner, M. Cheng, et al. (2012). Community seismic network, *Ann. Geophys.* **54**, no. 6, doi: [10.4401/ag-5269](https://doi.org/10.4401/ag-5269).
- Clayton, R. W., T. Heaton, M. Kohler, M. Chandy, R. Guy, and J. Bunn (2015). Community seismic network: A dense array to sense earthquake strong motion, *Seismol. Res. Lett.* **86**, no. 5, 1354–1363, doi: [10.1785/0220150094](https://doi.org/10.1785/0220150094).
- Clinton, J. F., and T. H. Heaton (2002). Potential advantages of a strong-motion velocity meter over a strong-motion accelerometer, *Seismol. Res. Lett.* **73**, no. 3, 332–342, doi: [10.1785/gssrl.73.3.332](https://doi.org/10.1785/gssrl.73.3.332).
- Cochran, E., J. Lawrence, C. Christensen, and A. Chung (2009). A novel strong-motion seismic network for community participation in earthquake monitoring, *IEEE Instrum. Meas. Mag.* **12**, no. 6, 8–15, doi: [10.1109/MIM.2009.5338255](https://doi.org/10.1109/MIM.2009.5338255).
- Cole, S., M. Karrenbach, D. Kahn, J. Rich, K. Silver, and D. Langton (2018). Source parameter estimation from DAS microseismic data, *SEG Technical Program Expanded Abstracts 2018*, Society of Exploration Geophysicists, 4928–4932.
- Correa, J., A. Egorov, K. Tertyshnikov, A. Bona, R. Pevzner, T. Dean, B. Freifeld, and S. Marshall (2017). Analysis of signal to noise and directivity characteristics of DAS VSP at near and far offsets—A CO2CRC Otway Project data example, *The Leading Edge* **36**, no. 12, 994a1–994a7, doi: [10.1190/tle36120994a1.1](https://doi.org/10.1190/tle36120994a1.1).
- Costa, L. D., H. F. Martins, S. Martin-Lopez, M. R. Fernandez-Ruiz, and M. Gonzalez-Herraez (2019). Fully distributed optical fiber strain sensor with $10^{-12} \text{ } \epsilon / \sqrt{\text{Hz}}$ sensitivity, *J. Lightwave Technol.* **37**, no. 18, 1–1, doi: [10.1109/JLT.2019.2904560](https://doi.org/10.1109/JLT.2019.2904560).
- Daley, T. M., B. M. Freifeld, J. Ajo-Franklin, S. Dou, R. Pevzner, V. Shulakova, S. Kashikar, D. E. Miller, J. Goetz, J. Hennings, et al. (2013). Field testing of fiber-optic distributed acoustic sensing (DAS) for subsurface seismic monitoring, *The Leading Edge* **32**, no. 6, 699–706, doi: [10.1190/tle32060699.1](https://doi.org/10.1190/tle32060699.1).
- Dean, T., T. Cuny, and A. H. Hartog (2017). The effect of gauge length on axially incident P-waves measured using fibre optic distributed vibration sensing: Gauge length effect on incident P-waves, *Geophys. Prospect.* **65**, no. 1, 184–193, doi: [10.1111/1365-2478.12419](https://doi.org/10.1111/1365-2478.12419).
- Dou, S., J. Ajo-Franklin, T. Daley, M. Robertson, T. Wood, B. Freifeld, R. Pevzner, J. Correa, K. Tertyshnikov, and M. Urosevic (2016). Surface orbital vibrator (SOV) and fiber-optic DAS: Field demonstration of economical, continuous-land seismic time-lapse monitoring from the Australian CO2CRC Otway site, *SEG Technical Program Expanded Abstracts 2016*, Society of Exploration Geophysicists, 5552–5556.
- Dou, S., N. Lindsey, A. M. Wagner, T. M. Daley, B. Freifeld, M. Robertson, J. Peterson, C. Ulrich, E. R. Martin, and J. B. Ajo-Franklin (2017). Distributed acoustic sensing for seismic monitoring of the near surface: A traffic-noise interferometry case study, *Sci. Rep.* **7**, Article Number 11620, doi: [10.1038/s41598-017-11986-4](https://doi.org/10.1038/s41598-017-11986-4).
- Fan, W., and J. J. McGuire (2018). Investigating microearthquake finite source attributes with IRIS community wavefield demonstration experiment in Oklahoma, *Geophys. J. Int.* **214**, no. 2, 1072–1087, doi: [10.1093/gji/ggy203](https://doi.org/10.1093/gji/ggy203).
- Farhadiroushan, M., T. Parker, S. Shatalin, A. Gillies, Z. Chen, A. Clarke, and G. Naldrett (2019). Practical reservoir monitoring using distributed acoustic sensor with engineered fiber, *Second EAGE Workshop Practical Reservoir Monitoring 2019*, Amsterdam, The Netherlands, 1–4 April, doi: [10.3997/2214-4609.201900006](https://doi.org/10.3997/2214-4609.201900006).
- Feigl, K. L., and P. Team (2017). *Overview and Preliminary Results from the PoroTomo Project at Brady Hot Springs, Nevada: Poroelastic Tomography by Adjoint Inverse Modeling of Data from Seismology, Geodesy, and Hydrology*, Proc. of the 42nd Workshop on Geothermal Reservoir Engineering, Stanford, California, 13–15.
- Feigl, K. L., L. M. Parker, and P. Team (2019). *PoroTomo Final Technical Report: Poroelastic Tomography by Adjoint Inverse Modeling of Data from Seismology, Geodesy, and Hydrology, 3.1*, doi: [10.2172/1499141](https://doi.org/10.2172/1499141).
- Frye, D., J. Ware, M. Grund, J. Partan, P. Koski, S. Singh, L. Freitag, J. Collins, and R. Detrick (2005). An acoustically-linked deep-ocean observatory, *Europe Oceans 2005*, IEEE, 969–974.
- Girard, S., J. Kuhnenn, A. Gusarov, B. Brichard, M. Van Uffelen, Y. Ouerdane, A. Boukenter, and C. Marcandella (2013). Radiation effects on silica-based optical fibers: Recent advances and future challenges, *IEEE Trans. Nuclear Sci.* **60**, no. 3, 2015–2036, doi: [10.1109/TNS.2012.2235464](https://doi.org/10.1109/TNS.2012.2235464).
- Graves, R., and A. Pitarka (2016). Kinematic ground-motion simulations on rough faults including effects of 3D stochastic velocity perturbations, *Bull. Seismol. Soc. Am.* **106**, no. 5, 2136–2153, doi: [10.1785/0120160088](https://doi.org/10.1785/0120160088).
- Gutscher, M.-A., J.-Y. Royer, D. Graindorge, S. Murphy, F. Klingelhoefer, A. Cattaneo, G. Barreca, L. Quétel, G. Riccobene, and F. Petersen (2018). Benefitting from cabled observatories to study active submarine faults: The FOCUS project (FOCUS = Fiber Optic Cable Use for Seafloor studies of earthquake hazard and deformation), *EGU General Assembly Conference Abstracts*, 7923.
- Hammond, J. O. S., R. England, N. Rawlinson, A. Curtis, K. Sigloch, N. Harmon, and B. Baptie (2019). The future of passive seismic acquisition, *Astron. Geophys.* **60**, no. 2, 2.37–2.42, doi: [10.1093/astrogeo/atz102](https://doi.org/10.1093/astrogeo/atz102).
- Hansen, S. M., B. Schmandt, A. Levander, E. Kiser, J. E. Vidale, G. A. Abers, and K. C. Creager (2016). Seismic evidence for a cold

- serpentinized mantle wedge beneath Mount St Helens, *Nature Comm.* **7**, Article Number 13242, doi: [10.1038/ncomms13242](https://doi.org/10.1038/ncomms13242).
- Harrison, J. C. (1976). Cavity and topographic effects in tilt and strain measurement, *J. Geophys. Res.* **81**, no. 2, 319–328, doi: [10.1029/JB081i002p00319](https://doi.org/10.1029/JB081i002p00319).
- Hartog, A. (1983). A distributed temperature sensor based on liquid-core optical fibers, *J. Lightwave Technol.* **1**, no. 3, 498–509, doi: [10.1109/JLT.1983.1072146](https://doi.org/10.1109/JLT.1983.1072146).
- Hartog, A. H. (2017). *An Introduction to Distributed Optical Fibre Sensors*, CRC press, Boca Raton, Florida.
- Hartog, A. H., M. Belal, and M. A. Clare (2018). Advances in distributed fiber-optic sensing for monitoring marine infrastructure, measuring the deep ocean, and quantifying the risks posed by seafloor hazards, *Mar. Technol. Soc. J.* **52**, no. 5, 58–73, doi: [10.4031/MTSJ.52.5.7](https://doi.org/10.4031/MTSJ.52.5.7).
- Hartog, A. H., O. I. Kotov, and L. B. Liokumovich (2013). The optics of distributed vibration sensing, *Second EAGE Workshop on Permanent Reservoir Monitoring 2013—Current and Future Trends*, doi: [10.3997/2214-4609.20131301](https://doi.org/10.3997/2214-4609.20131301).
- Hornman, J. C. (2017). Field trial of seismic recording using distributed acoustic sensing with broadside sensitive fibre-optic cables: Field trial of seismic recording, *Geophys. Prospect.* **65**, no. 1, 35–46, doi: [10.1111/1365-2478.12358](https://doi.org/10.1111/1365-2478.12358).
- Huot, F., and B. Biondi (2018). Machine learning algorithms for automated seismic ambient noise processing applied to DAS acquisition, *SEG Technical Program Expanded Abstracts 2018*, Society of Exploration Geophysicists, 5501–5505.
- Ikuta, R. (2002). Continuous monitoring of propagation velocity of seismic wave using ACROSS, *Geophys. Res. Lett.* **29**, no. 13, doi: [10.1029/2001GL013974](https://doi.org/10.1029/2001GL013974).
- Inbal, A., J. P. Ampuero, and R. W. Clayton (2016). Localized seismic deformation in the upper mantle revealed by dense seismic arrays, *Science* **354**, no. 6308, 88–92.
- Inbal, A., Q. Kong, W. Savran, and R. M. Allen (2019). On the feasibility of using the dense MyShake smartphone array for earthquake location, *Seismol. Res. Lett.* **90**, no. 3, 1209–1218, doi: [10.1785/0220180349](https://doi.org/10.1785/0220180349).
- Iten, M. (2011). Novel applications of distributed fiber-optic sensing in geotechnical engineering, *Doctoral Thesis*, ETH Zurich, doi: [10.3929/ethz-a-6559858](https://doi.org/10.3929/ethz-a-6559858).
- Jousset, P., T. Reinsch, T. Ryberg, H. Blanck, A. Clarke, R. Aghayev, G. P. Hersir, J. Hennings, M. Weber, and C. M. Krawczyk (2018). Dynamic strain determination using fibre-optic cables allows imaging of seismological and structural features, *Nature Comm.* **9**, Article Number 2509, doi: [10.1038/s41467-018-04860-y](https://doi.org/10.1038/s41467-018-04860-y).
- Karplus, M., and B. Schmandt (2018). Preface to the focus section on geophone array seismology, *Seismol. Res. Lett.* **89**, no. 5, 1597–1600.
- Karrenbach, M., S. Cole, A. Ridge, K. Boone, D. Kahn, J. Rich, K. Silver, and D. Langton (2018). Fiber-optic distributed acoustic sensing of microseismicity, strain and temperature during hydraulic fracturing, *Geophysics* **84**, no. 1, D11–D23.
- Karrenbach, M. H., and S. Cole (2016). Distributed fiber optic sensors for earthquake detection and early warning, *AGU Fall Meeting Abstracts*, Abstract S51D–02.
- Kiser, E., A. Levander, C. Zelt, B. Schmandt, and S. Hansen (2018). Focusing of melt near the top of the Mount St. Helens (USA) magma reservoir and its relationship to major volcanic eruptions, *Geology* **46**, no. 9, 775–778.
- Kobs, S., D. M. Holland, V. Zagorodnov, A. Stern, and S. W. Tyler (2014). Novel monitoring of Antarctic ice shelf basal melting using a fiber-optic distributed temperature sensing mooring: Novel monitoring of antarctic ice shelf, *Geophys. Res. Lett.* **41**, no. 19, 6779–6786, doi: [10.1002/2014GL061155](https://doi.org/10.1002/2014GL061155).
- Kong, Q., R. M. Allen, L. Schreier, and Y.-W. Kwon (2016). MyShake: A smartphone seismic network for earthquake early warning and beyond, *Sci. Adv.* **2**, no. 2, e1501055, doi: [10.1126/sciadv.1501055](https://doi.org/10.1126/sciadv.1501055).
- Kuvshinov, B. N. (2016). Interaction of helically wound fibre-optic cables with plane seismic waves: Interaction of fibre-optic cables, *Geophys. Prospect.* **64**, no. 3, 671–688, doi: [10.1111/1365-2478.12303](https://doi.org/10.1111/1365-2478.12303).
- Lancelle, C. (2016). Distributed acoustic sensing for imaging near-surface geology and monitoring traffic at Garner Valley, California, *Ph.D. Thesis*, The University of Wisconsin-Madison.
- Lapusta, N., E. Dunham, J.-P. Avouac, M. Denolle, Y. v. Dinther, D. Faulkner, Y. Fialko, H. Kitajima, V. Lambert, S. Laroche, et al. (2019). *Modeling Earthquake Source Processes: from Tectonics to Dynamic Rupture*, Report to the National Science Foundation.
- Lellouch, A., S. Yuan, Z. Spica, B. Biondi, and W. L. Ellsworth (2019). Seismic velocity estimation using passive downhole distributed acoustic sensing records—Examples from the San Andreas fault observatory at depth, *J. Geophys. Res.* **124**, no. 7, doi: [10.1029/2019JB017533](https://doi.org/10.1029/2019JB017533).
- Li, C., Z. Li, Z. Peng, C. Zhang, N. Nakata, and T. Sickbert (2018). Long-period long-duration events detected by the IRIS community wavefield demonstration experiment in Oklahoma: Tremor or train signals? *Seismol. Res. Lett.* **89**, no. 5, 1652–1659, doi: [10.1785/0220180081](https://doi.org/10.1785/0220180081).
- Li, Z., and Z. Zhan (2018). Pushing the limit of earthquake detection with distributed acoustic sensing and template matching: A case study at the Brady geothermal field, *Geophys. J. Int.* **215**, no. 3, 1583–1593, doi: [10.1093/gji/ggy359](https://doi.org/10.1093/gji/ggy359).
- Li, Z., Z. Peng, D. Hollis, L. Zhu, and J. McClellan (2018). High-resolution seismic event detection using local similarity for large-*N* arrays, *Sci. Rep.* **8**, no. 1, Article Number 1646.
- Li, Z., Z. Zhan, M. Kohler, and E. Hauksson (2019). Quantitative assessment of earthquake detection capability of DAS, MEMS and broadband networks in Pasadena, CA, *2019 SSA Annual Meeting*, Seattle, Washington, 27–30 April.
- Lim Chen Ning, I., and P. Sava (2018). High-resolution multi-component distributed acoustic sensing: Hi-res multi-component DAS, *Geophys. Prospect.* **66**, no. 6, 1111–1122, doi: [10.1111/1365-2478.12634](https://doi.org/10.1111/1365-2478.12634).
- Lin, F.-C., D. Li, R. W. Clayton, and D. Hollis (2013). High-resolution 3D shallow crustal structure in Long Beach, California: Application of ambient noise tomography on a dense seismic array, *Geophysics* **78**, no. 4, Q45–Q56.
- Lindsey, N., C. Dawe, and J. Ajo-Franklin (2019). Photonic seismology in Monterey Bay: Dark fiber DAS illuminates offshore faults and coastal ocean dynamics, *EarthArXiv*, doi: [10.31223/osf.io/7bf92](https://doi.org/10.31223/osf.io/7bf92).
- Lindsey, N. J., E. R. Martin, D. S. Dreger, B. Freifeld, S. Cole, S. R. James, B. L. Biondi, and J. B. Ajo-Franklin (2017). Fiber-optic network observations of earthquake wavefields: Fiber-optic earthquake observations, *Geophys. Res. Lett.* **44**, no. 23, 11,792–11,799, doi: [10.1002/2017GL075722](https://doi.org/10.1002/2017GL075722).
- Marra, G., C. Clivati, R. Lockett, A. Tampellini, J. Kronjäger, L. Wright, A. Mura, F. Levi, S. Robinson, A. Xuereb, et al. (2018).

- Ultrastable laser interferometry for earthquake detection with terrestrial and submarine cables, *Science* **361**, no. 6401, doi: [10.1126/science.aat4458](https://doi.org/10.1126/science.aat4458).
- Martin, E. R., F. Huot, Y. Ma, R. Cieplicki, S. Cole, M. Karrenbach, and B. L. Biondi (2018). A seismic shift in scalable acquisition demands new processing: Fiber-Optic seismic signal retrieval in urban areas with unsupervised learning for coherent noise removal, *IEEE Signal Process. Mag.* **35**, no. 2, 31–40, doi: [10.1109/MSP.2017.2783381](https://doi.org/10.1109/MSP.2017.2783381).
- Martin, E. R., N. Lindsey, J. Ajo-Franklin, and B. Biondi (2019). Introduction to interferometry of fiber optic strain measurements, *EarthArXiv*, preprint, doi: [10.31223/osf.io/s2tjd](https://doi.org/10.31223/osf.io/s2tjd).
- Masoudi, A., and T. P. Newson (2016). Contributed review: Distributed optical fibre dynamic strain sensing, *Rev. Scientific Inst.* **87**, no. 1, 011501, doi: [10.1063/1.4939482](https://doi.org/10.1063/1.4939482).
- Mateeva, A., J. Lopez, J. Mestayer, P. Wills, B. Cox, D. Kiyashchenko, Z. Yang, W. Berlang, R. Detomo, and S. Grandi (2013). Distributed acoustic sensing for reservoir monitoring with VSP, *The Leading Edge* **32**, no. 10, 1278–1283, doi: [10.1190/le32101278.1](https://doi.org/10.1190/le32101278.1).
- Mateeva, A., J. Lopez, H. Potters, J. Mestayer, B. Cox, D. Kiyashchenko, P. Wills, S. Grandi, K. Hornman, B. Kuvshinov, et al. (2014). Distributed acoustic sensing for reservoir monitoring with vertical seismic profiling: Distributed acoustic sensing (DAS) for reservoir monitoring with VSP, *Geophys. Prospect.* **62**, no. 4, 679–692, doi: [10.1111/1365-2478.12116](https://doi.org/10.1111/1365-2478.12116).
- Meng, H., and Y. Ben-Zion (2018). Detection of small earthquakes with dense array data: Example from the San Jacinto fault zone, southern California, *Geophys. J. Int.* **212**, no. 1, 442–457, doi: [10.1093/gji/ggx404](https://doi.org/10.1093/gji/ggx404).
- Mestayer, J., B. Cox, P. Wills, D. Kiyashchenko, J. Lopez, M. Costello, S. Bourne, G. Ugueto, R. Lupton, and G. Solano (2011). Field trials of distributed acoustic sensing for geophysical monitoring, *SEG Technical Program Expanded Abstracts 2011*, Society of Exploration Geophysicists, 4253–4257.
- Nakata, N., J. P. Chang, J. F. Lawrence, and P. Boué (2015). Body wave extraction and tomography at Long Beach, California, with ambient-noise interferometry, *J. Geophys. Res.* **120**, no. 2, 1159–1173.
- Nolet, G., Y. Hello, S. van der Lee, S. Bonnieux, M. C. Ruiz, N. A. Pazmino, A. Deschamps, M. M. Regnier, Y. Font, Y. J. Chen, et al. (2019). Imaging the Galápagos mantle plume with an unconventional application of floating seismometers, *Sci. Rep.* **9**, no. 1, doi: [10.1038/s41598-018-36835-w](https://doi.org/10.1038/s41598-018-36835-w).
- Paitz, P., K. Sager, and A. Fichtner (2019). Rotation and strain ambient noise interferometry, *Geophys. J. Int.* **216**, no. 3, 1938–1952, doi: [10.1093/gji/ggy528](https://doi.org/10.1093/gji/ggy528).
- Papp, B., D. Donno, J. E. Martin, and A. H. Hartog (2017). A study of the geophysical response of distributed fibre optic acoustic sensors through laboratory-scale experiments: Geophysical response of fibre optic sensors, *Geophys. Prospect.* **65**, no. 5, 1186–1204, doi: [10.1111/1365-2478.12471](https://doi.org/10.1111/1365-2478.12471).
- Parker, L. M., C. H. Thurber, X. Zeng, P. Li, N. E. Lord, D. Fratta, H. F. Wang, M. C. Robertson, A. M. Thomas, M. S. Karplus, et al. (2018). Active-source seismic tomography at the Brady geothermal field, Nevada, with dense nodal and fiber-optic seismic arrays, *Seismol. Res. Lett.* **89**, no. 5, 1629–1640, doi: [10.1785/0220180085](https://doi.org/10.1785/0220180085).
- Parker, T., S. Shatalin, and M. Farhadiroushan (2014). Distributed acoustic sensing—A new tool for seismic applications, *First Break* **32**, 9.
- Peng, Z., and P. Zhao (2009). Migration of early aftershocks following the 2004 Parkfield earthquake, *Nature Geosci.* **2**, no. 12, 877–881, doi: [10.1038/ngeo697](https://doi.org/10.1038/ngeo697).
- Podolskiy, E. A., and F. Walter (2016). Cryoseismology, *Rev. Geophys.* **54**, no. 4, 708–758, doi: [10.1002/2016rg000526](https://doi.org/10.1002/2016rg000526).
- Ross, Z. E., D. T. Trugman, E. Hauksson, and P. M. Shearer (2019). Searching for hidden earthquakes in Southern California, *Science* **364**, no. 6442, doi: [10.1126/science.aaw6888](https://doi.org/10.1126/science.aaw6888).
- Ross, Z. E., Y. Yue, M.-A. Meier, E. Hauksson, and T. H. Heaton (2019). PhaseLink: A deep learning approach to seismic phase association, *J. Geophys. Res.* **124**, no. 1, 856–869, doi: [10.1029/2018JB016674](https://doi.org/10.1029/2018JB016674).
- Schmandt, B., and R. W. Clayton (2013). Analysis of teleseismic *P* waves with a 5200-station array in Long Beach, California: Evidence for an abrupt boundary to Inner Borderland rifting, *J. Geophys. Res.* **118**, no. 10, 5320–5338.
- Shelly, D. R., G. C. Beroza, and S. Ide (2007). Non-volcanic tremor and low-frequency earthquake swarms, *Nature* **446**, no. 7133, 305–307, doi: [10.1038/nature05666](https://doi.org/10.1038/nature05666).
- Shi, J., and D. Asimaki (2018). A generic velocity profile for basin sediments in California conditioned on V_{S30} , *Seismol. Res. Lett.* **89**, no. 4, 1397–1409, doi: [10.1785/0220170268](https://doi.org/10.1785/0220170268).
- Sladen, A., D. Rivet, J.-P. Ampuero, L. De Barros, Y. Hello, G. Calbris, and P. Lamare (2019). Distributed sensing of earthquakes and ocean-solid Earth interactions on seafloor telecom cables, *EarthArXiv*, doi: [10.31223/osf.io/ekrfy](https://doi.org/10.31223/osf.io/ekrfy).
- Sweet, J. R., K. R. Anderson, S. Bilek, M. Brudzinski, X. Chen, H. DeShon, C. Hayward, M. Karplus, K. Keranen, C. Langston, et al. (2018). A community experiment to record the full seismic wavefield in Oklahoma, *Seismol. Res. Lett.* **89**, no. 5, 1923–1930, doi: [10.1785/0220180079](https://doi.org/10.1785/0220180079).
- Tanimoto, T., and T. Okamoto (2014). The Millikan shaking experiments and high-frequency seismic wave propagation in Southern California, *Geophys. J. Int.* **198**, no. 2, 1081–1095, doi: [10.1093/gji/ggu189](https://doi.org/10.1093/gji/ggu189).
- University of Wisconsin (2017). PoroTomo Natural Laboratory horizontal distributed acoustic sensing data, data set, available at <http://gdr.openei.org/submissions/980> (last accessed May 2019).
- Wald, D. J., V. Quitoriano, T. H. Heaton, H. Kanamori, C. W. Scrivner, and C. B. Worden (1999). TriNet ShakeMaps: Rapid generation of peak ground motion and intensity maps for earthquakes in southern California, *Earthq. Spectra* **15**, no. 3, 537–555.
- Wang, H., X. Comas, and S. Tyler (2019). Fiber-optic networks find a new use as seismic sensor arrays, *Eos Trans. AGU* **100**, doi: [10.1029/2019EO119897](https://doi.org/10.1029/2019EO119897).
- Wang, H. F., X. Zeng, D. E. Miller, D. Fratta, K. L. Feigl, C. H. Thurber, and R. J. Mellors (2018). Ground motion response to an M_L 4.3 earthquake using co-located distributed acoustic sensing and seismometer arrays, *Geophys. J. Int.* **213**, no. 3, 2020–2036, doi: [10.1093/gji/ggy102](https://doi.org/10.1093/gji/ggy102).
- Williams, E. F., M. R. Fernandez-Ruiz, R. Magalhaes, R. Vanthillo, Z. Zhan, M. Gonzalez-Herraez, and H. F. Martins (2019). Teleseisms and microseisms on an ocean-bottom distributed acoustic sensing array, *EarthArXiv*, doi: [10.31223/osf.io/kg7q4](https://doi.org/10.31223/osf.io/kg7q4).
- Williams, E. F., Z. Zhan, M. Karrenbach, S. Cole, and L. LaFlame (2019). High-resolution mapping and monitoring of shallow shear-wave velocity in Urban Pasadena with distributed acoustic sensing, *2019 SSA Annual Meeting*, Seattle, Washington, 27–30 April.

- Willis, M., J. Ajo-Franklin, and B. Roy (2017). Introduction to this special section: Geophysical applications of fiber-optic distributed sensing, *The Leading Edge* **36**, no. 12, 973–974.
- Worden, C. B., D. J. Wald, T. I. Allen, K. Lin, D. Garcia, and G. Cua (2010). A revised ground-motion and intensity interpolation scheme for ShakeMap, *Bull. Seismol. Soc. Am.* **100**, no. 6, 3083–3096, doi: [10.1785/0120100101](https://doi.org/10.1785/0120100101).
- Yong, A., E. M. Thompson, D. J. Wald, K. L. Knudsen, J. K. Odum, W. J. Stephenson, and S. Haefner (2016). Compilation of V_{S30} Data for the United States, *U.S. Geological Survey Data Series 978*, 8 pp.
- Yu, C., Z. Zhan, N. J. Lindsey, J. B. Ajo-Franklin, and M. Robertson (2019). The potential of DAS in teleseismic studies: Insights from the goldstone experiment, *Geophys. Res. Lett.* **46**, no. 3, 1320–1328, doi: [10.1029/2018GL081195](https://doi.org/10.1029/2018GL081195).
- Zeng, X., C. Lancelle, C. Thurber, D. Fratta, H. Wang, N. Lord, A. Chalari, and A. Clarke (2017). Properties of noise cross-correlation functions obtained from a distributed acoustic sensing array at Garner Valley, California, *Bull. Seismol. Soc. Am.* **107**, no. 2, 603–610, doi: [10.1785/0120160168](https://doi.org/10.1785/0120160168).
- Zeng, X., C. Thurber, H. Wang, D. Fratta, E. Matzel, and P. Team (2017). High-resolution shallow structure revealed with ambient noise tomography on a dense array, *42nd Workshop Geothermal Reservoir Engineering*, Stanford, California, 13–15 February, 6 pp.
- Zhan, G., Y. Li, A. Tura, M. Willis, and E. Martin (2019). Introduction to special section: Distributed acoustic sensing and its oilfield potential, *Interpretation* **7**, no. 1, doi: [10.1190/INT-2019-0116-SPSEINTRO.1](https://doi.org/10.1190/INT-2019-0116-SPSEINTRO.1).
- Zhu, W., and G. C. Beroza (2018). PhaseNet: A deep-neural-network-based seismic arrival time picking method, *Geophys. J. Int.* **216**, no. 1, 261–273, doi: [10.1093/gji/ggy423](https://doi.org/10.1093/gji/ggy423).
-

Manuscript received 12 May 2019
Published online 4 December 2019